[^{99m}Tc]Demotate, a new ^{99m}Tc-based [Tyr^3]octreotate analogue for the detection of somatostatin receptor-positive tumours: synthesis and preclinical results

Theodosia Maina[1], Berthold Nock[1], Anastasia Nikolopoulou[1], Petros Sotiriou[2], George Loudos[3], Dimitrios Maintas[4], Paul Cordopatis[2], Efstratios Chiotellis[5]

[1] Institute of Radioisotopes – Radiodiagnostic Products, National Center for Scientific Research "Demokritos", 15310 Ag. Paraskevi, Attikis, Athens, Greece
[2] Department of Pharmacy, University of Patras, 26500 Patras, Greece
[3] National Technical University of Athens, 15773 Zografou, Athens, Greece
[4] Institute for Isotopic Studies, 15125 Maroussi, Athens, Greece
[5] Department of Pharmacy, University of Thessaloniki, 54006 Thessaloniki, Greece

Received 17 November 2001 and in revised form 24 January 2002 / Published online: 23 March 2002

Abstract. Demotate is a new tetraamine-functionalised [Tyr^3]octreotate derivative that binds technetium-99m with a high efficiency under mild conditions. The resulting radioligand, [^{99m}Tc]Demotate, forms in a high purity and is stable for at least 6 h after labelling. The affinity of the unlabelled peptide for somatostatin receptors is high (IC_{50}=0.13 n*M*) and comparable to that of [Tyr^3]octreotate or [Tyr^3]octreotide, as demonstrated by competition binding experiments in rat brain cortex or AR42J cell membrane preparations. An equally very high affinity (K_d=0.07 n*M*) was exhibited by [^{99m}Tc/^{99g}Tc]Demotate during saturation binding experiments using rat brain cortex membrane homogenates. The radioligand resisted hydrolytic degradation in mouse plasma and was excreted intact in mouse urine. In vivo, [^{99m}Tc]Demotate cleared very rapidly from non-target tissues into the bladder via the kidneys, while radioactivity uptake in target organs was very high. In mice bearing the experimental AR42J tumour, [^{99m}Tc]Demotate demonstrated a very high tumour uptake at 1 h p.i. (25%ID/g) that remained high (20%ID/g) at 4 h p.i. This uptake could be effectively blocked by co-injection of a high dose of [Tyr^3]octreotate together with the radioligand. High-quality planar and single-photon emission tomographic images were acquired 1 h after injection of [^{99m}Tc]Demotate in tumour-bearing mice, illustrating the excellent properties of this agent for somatostatin receptor tumour imaging.

Theodosia Maina (✉)
Institute of Radioisotopes – Radiodiagnostic Products,
National Center for Scientific Research "Demokritos",
15310 Ag. Paraskevi, Attikis, Athens, Greece
e-mail: mainathe@mail.demokritos.gr
Tel.: +30-10-650-3908, Fax: +30-10-6524480

Keywords: Somatostatin receptor – Tumour imaging – ^{99m}Tc – [Tyr^3]octreotate – Tetraamine chelator

Abbreviations. Tetraamine = N_4 = 6-*R*-1,4,8,11-tetraazaundecane, *R* = coupling group; Demotate = [N_4^0,Tyr^3]octreotate, with *R*=CO; HYNIC = hydrazinonicotinamide; tricine = *N*-[tris(hydroxymethyl)methyl]glycine; EDDA = ethylenediamine-*N*,*N*´-diacetic acid; [Tyr^3]octreotide = H-(D)Phe-Cys-Tyr-(D)Trp-Lys-Thr-Cys-Thr(ol); [Tyr^3]octreotate = H-(D)Phe-Cys-Tyr-(D)Trp-Lys-Thr-Cys-Thr-OH; SPET = single-photon emission tomography; DTPA = diethylene triamine pentaacetic acid; HPLC = high-performance liquid chromatography

Eur J Nucl Med (2002) 29:742–753
DOI 10.1007/s00259-002-0782-9

Introduction

The past decade has witnessed spectacular growth in the development of small radiolabelled peptides for use in the scintigraphic imaging of high-affinity tumour-associated receptors [1, 2, 3, 4, 5, 6]. Evidence on the overexpression of somatostatin receptors by primary and metastatic malignant disease, mainly of neuroendocrine origin, has prompted a worldwide search for radiolabelled somatostatin analogues for use in somatostatin receptor-mediated tumour imaging (SRI) [6, 7, 8]. Soon after the first report on the successful visualisation of somatostatin receptor-positive neoplastic lesions with a radioiodinated synthetic somatostatin analogue ([^{123}I-Tyr^3]octreo-

tide) [9], an improved octreotide-based radioligand labelled with indium-111 was introduced [10]. Thus, the first radiopharmaceutical for the SRI of neuroendocrine tumours, [^{111}In-DTPA^{0}]octreotide ([^{111}In]OctreoScan), was approved and became available [6]. Today SRI with [^{111}In]OctreoScan is considered a very powerful non-invasive technique for the localisation and staging of neuroendocrine tumours. However, wider application of [^{111}In]OctreoScan in diagnostic oncology is restricted by the high cost and limited availability of the cyclotron-produced ^{111}In and its suboptimal nuclear characteristics, such as the medium-energy photons (171 keV, 245 keV), which lead to a poor image resolution and a high radiation dose to the patient. Similar efforts involving somatostatin analogues labelled with alternative diagnostic radionuclides led to radioligands equally hampered by drawbacks related to commercial availability, physical half-life or the photon energy of the radionuclides [6].

As a consequence, the search for a technetium-99m-based somatostatin analogue has been intensified recently [3, 5]. This effort is warranted by the fact that ^{99m}Tc still dominates nuclear medicine diagnosis as a result of its superior nuclear characteristics (half-life of 6 h and monoenergetic gamma radiation of 141 keV), which minimise the radiation exposure of the patient while providing high-resolution images with currently available instrumentation [3, 5]. On the other hand, the wide availability and cost-effectiveness of ^{99m}Tc are of major importance for routine clinical applications. Moreover, it is now generally recognised that the rapid blood clearance and fast target localisation properties of small peptides, such as octreotide or other somatostatin analogues, are best taken into account when short-lived radionuclides, like ^{99m}Tc, are employed [3, 5]. As a result, over the past few years several somatostatin analogues have emerged that carry a variety of chelators for efficient ^{99m}Tc labelling, such as diamidedithiols, triamidethiols, aminediamidethiols [11, 12, 13, 14], propylene amine oxime [15], open chain or cyclic tetraamines [16, 17] and HYNIC in combination with different co-ligands [14, 18, 19, 20].

As a continuation of previous work [15, 16], we report here on the synthesis, radiochemistry and biological evaluation of [N_4^0,Tyr^3]octreotate labelled with ^{99m}Tc, [^{99m}Tc]Demotate. In this new compound, [Tyr^3]octreotate carries at the N-terminal an open chain tetraamine that serves as the ^{99m}Tc binding site. [Tyr^3]octreotate was selected as the receptor recognition site on the basis of recent data on the improved tumour localisation properties of [Tyr^3]octreotate-based radioligands as compared with those based on octreotide [4, 6, 21, 22]. In addition, a [Tyr^3]octreotate-based radioligand is expected to clear more rapidly from non-target tissues as a result of the extra carboxylic group at the C-terminal of the peptide. Labelling with ^{99m}Tc is reported, along with results of experiments with cell preparations and animal models demonstrating the very promising characteristics of [^{99m}Tc]Demotate for SRI applications. Preliminary studies with [^{99m}Tc]Demotate involving a small number of carcinoid and pancreatic carcinoma patients have already been initiated and preclinical data are presented here.

Materials and methods

General

Unless otherwise stated, all chemicals were reagent grade and used without further purification. Synthesis of the Boc-protected tetraamine precursor N,N′,N″,N‴-tetra-(*tert*-butoxycarbonyl)-6-(carboxy)-1,4,8,11-tetraazaundecane will be reported elsewhere. [Tyr^3]octreotide was kindly provided by the International Atomic Energy Agency. [Tyr^3]octreotate was synthesised on the solid phase, as described below. Iodine-125 was purchased from MDS Nordion, SA (Fleurus, Belgium). Radiiodination of [Tyr^3]octreotide was performed according to described methods [23]. Technetium-99m was used as a [^{99m}Tc]$NaTcO_4$ solution in physiological saline, eluted from a commercial ^{99}Mo/^{99m}Tc generator (Cis International). Technetium-99g was purchased from Oak Ridge National Laboratories, USA, as $NH_4{}^{99g}TcO_4$. The impure black solid was purified prior to use by overnight treatment with H_2O_2 and NH_4OH in MeOH. Evaporation of the solvent afforded $NH_4{}^{99g}TcO_4$ as a white powder. Solvents for high-performance liquid chromatography (HPLC) were HPLC grade; they were filtered through 0.22-µm membrane filters (Millipore, Milford/USA) and degassed by helium flux prior to use.

HPLC analyses were performed on a Waters Chromatograph efficient with a 600 solvent delivery system and coupled to both a Waters 996 photodiode array UV detector and a Gabi gamma detector from Raytest (RSM Analytische Instrumente GmbH, Germany). The Millennium Software by Waters was applied for controlling the HPLC system and processing the data. The RP Symmetry Shield column from Waters was used (5 µm, 3.9 mm×150 mm), applying the elution systems described in the text. Paper chromatography was conducted on Whatman 3-mm paper strips. For radioactivity measurements, an automatic well-type gamma counter calibrated for ^{99m}Tc was used [NaI(Tl) crystal, Canberra Packard Auto-Gamma 5000 series instrument]. A Brandel M-48 Cell Harvester was employed in binding experiments. For imaging, a small field of view experimental gamma camera, suitable for both planar and tomographic imaging, was employed. The system is based on a position-sensitive photomultiplier tube (Hamamatsu R2486), a pixelised CsI(Tl) scintillation crystal and CAMAC electronics [24, 25].

The rat pancreatic tumour cell line AR42J was kindly provided by Dr. R. Kleene (Philipps University, Marburg, Germany) and Dr. S. Mather (St. Bartholomew's Hospital, London, UK). All culture media were supplied by Gibco BRL, Life Technologies (Grand Island, N.Y.) and all supplements by Biochrom KG Seromed (Berlin, Germany). For protein measurements the protein microdetermination kit (Procedure No. P 5656) produced by Sigma Diagnostics (St. Louis, USA) was utilised. Animal experiments were carried out in compliance with European and national regulations. In-house male Wistar rats (200±10 g) were used for the preparation of cortex membranes. For biodistribution experiments, in-house male Swiss albino mice (30±5 g) were used. For experimental tumour models, female Swiss-nu/nu mice of 7 weeks of age on arrival (Iffa Credo, France) were employed, and the animals were kept under aseptic conditions until biodistribution was studied.

Synthesis of Demotate

The [Tyr^3]octreotate amino acid sequence (D)Phe-Cys-Tyr-(D)Trp-Lys-Thr-Cys-Thr-OH was built on the acid-sensitive 2-chlorotrityl chloride resin [26] (substitution 0.6 mmol/g) applying the fmoc strategy [27, 28]. The following side chain-protected amino acids were used: Fmoc-Cys(Mmt), Fmoc-Tyr(^{t}Bu), Fmoc-Thr(^{t}Bu), Fmoc-Lys(Boc), Fmoc-(D)Trp(Boc). Coupling of each amino acid was performed with a 3 molar excess of N^{α}-fluorenylmethyloxycarbonyl-amino acid, 4.5 molar excess of HOBt (1-hydroxybenotriazol) and 3.3 molar excess of DIC (diisopropylcarbodiimide) in DMF for 3 h. The reaction was monitored by the ninhydrin test and the Fmoc groups were removed by treatment with 20% piperidine in DMF for 30 min. Finally, N,N′,N″,N‴-tetra-(*tert*-butoxycarbonyl)-6-(carboxy)-1,4,8,11-tetraazaundecane was coupled to the terminal (D)Phe of the resin-immobilised peptide. For coupling, a 3 molar excess of Boc-protected tetraamine, 3.3 molar excess of *O*-(7-azabenzotriazolyl-1,1,3,3-tetramethylammonium hexafluorophosphate (HATU) and 7 molar excess of diisopropylamine in DMF were reacted for 2 h [28]. Cleavage of the tetraamine-modified peptide chain from the resin and removal of lateral protecting groups was achieved by a 5-h treatment in a solution of trifluoroacetic acid/DCM/1,2-ethanedithiol/water/anisole (8/1/0.7/0.2/0.1, 20 ml/g peptide resin) at ambient temperature. The solution was concentrated to a small volume and the peptide precipitated with ether. It was cyclised by 72-h treatment with a 20% DMSO aqueous solution (3 ml/mg peptide) at ambient temperature. The resulting crude product containing [N_4^0, Tyr^3]octreotate, Demotate, was subjected to gel chromatography on Sephadex G-15 using 0.2 *M* acetic acid as the eluent. In this way, sample desalting was achieved along with removal of low molecular weight contaminants (e.g. scavengers). Final purification was achieved by semipreparative HPLC on a RP C-18 support (Phase Sep C-18 S10 ODS2) eluted with a linear gradient 10% to 80% acetonitrile (0.1% TFA) over 30 min at a 2 ml/min flow rate.

Overall yield: 37%; TLC R_f (SiO_2 type G_{60}-F_{254}, Merck; 1-butanol/acetic acid/H_2O/pyridine 15/3/10/6): 0.3; UV/RP-HPLC t_R (Techsphere 5 ODS2 C-18 250 mm×4.6 mm column from HPLC Technology, applying the above-described linear gradient system): 16 min; ES-MS: 1235.5 (M^+, 100), 618.4 (MH^{2+}, 35).

Radiolabelling of Demotate with ^{99m}Tc

Lyophilised Demotate was dissolved in 10 m*M* acetic acid at a final 1 m*M* concentration. The bulk solution was distributed in 50-µl aliquots in Eppendorf vials that were stored at –20°C. To an Eppendorf vial containing 0.5 *M* phosphate buffer pH 11.5 (50 µl) the following solutions were consecutively added: 0.1 *M* sodium citrate (5 µl), pertechnetate generator eluate (405 µl, 5–10 mCi), Demotate stock solution (15 µl) and finally a freshly prepared ethanolic $SnCl_2$ solution (25 µg, 25 µl). The mixture was left to react for 30 min at ambient temperature and then it was neutralised by the addition of 1 *M* HCl (10 µl).

Quality control

Aliquots (1 µl) of the labelling solution were analysed by HPLC applying a linear gradient system at a 1.0 ml/min flow rate from 0% B to 60% B in 30 min, where solvent A = 0.1% trifluoroacetic acid in water and solvent B = pure acetonitrile. Under these conditions, [^{99m}Tc]Demotate elutes at 18.1 min, [^{99m}Tc]citrate at 1.4–1.8 min and $^{99m}TcO_4^-$ at 3.8 min. For detection of any reduced hydrolysed technetium present ($^{99m}TcO_2$), paper chromatography was conducted. An aliquot (<1 µl) of the labelled product was applied on the paper strip that was developed up to 10 cm from the origin with 1 *M* ammonium acetate/pure MeOH 1/1 (v/v). The paper was left to dry in the open and then cut into two pieces: 1st = Start (origin +0.5–1 cm): $^{99m}TcO_2$ and 2nd = Front (the rest of the strip): $^{99m}TcO_4^-$, [^{99m}Tc]citrate and [^{99m}Tc]Demotate. The radioactivity content of each piece was measured in the gamma counter. Stability tests of the radiolabelled product were conducted up to 6 h post labelling.

Cell culture

Rat pancreatic carcinoma AR42J cells were grown confluent in F-12 K nutrient mixture supplemented by 10% (v/v) fetal bovine serum, 1 m*M* glutamine, 100 U/ml penicillin and 100 µg/ml streptomycin in humidified air containing 5% CO_2 at 37°C. Subculturing was performed employing a trypsin/EDTA (0.05%/0.02% w/v) solution.

Membrane preparation

Membrane preparation from rat brain cortex. Rat brain cortex membranes were prepared using a modified published method [29]. Briefly, brain cortex from three Wistar rats was dissected and immediately placed in ice-cold Hank's balanced salt solution (HBSS) pH 7.5 supplemented with 50 µl/ml penicillin, 50 µg/ml streptomycin and 10,000 KIU/l aprotinin. The cortex was then rinsed twice with ice-cold HBSS solution and minced with a surgical blade. The fine, uniform aggregate suspension was then centrifuged at 500 *g* for 10 min at 4°C in a J2-MC Beckman centrifuge and the pellet was homogenised in 20 ml homogenisation buffer consisting of 25 m*M* Tris buffer pH 7.5, 0.3 *M* sucrose, 0.25 m*M* PMSF, 1 m*M* EGTA and 10,000 KIU/l aprotinin, using a 10-ml syringe. The homogenate was centrifuged as described above and the pellet was homogenised three more times in the same way, saving the supernatant after each centrifugation. The combined supernatants were then centrifuged at 48,000 *g* for 45 min at 4°C in a CS120GX micro ultracentrifuge (Hitachi). The final pellet was washed twice with 50 m*M* Tris buffer pH 7.5 containing 5 m*M* $MgCl_2$, 20 mg/l bacitracin, 0.25 m*M* PMSF, 10,000 KIU/l aprotinin and 100 IU/ml RNase inhibitor and resuspended in 5 ml of washing buffer, separated into 100-µl aliquots and stored immediately at –80°C.

Membrane preparation from AR42J cells. AR42J cells were grown to confluence, mechanically disaggregated, washed twice with cold PBS buffer pH 7.0 and resuspended in homogenisation buffer (1 ml/flask) containing 10 m*M* Tris pH 7.4 and 0.1 m*M* EDTA (Dr. Z. Georgoussi, personal communication). Cells were homogenised using a Bioblock Scientific homogeniser (50 strokes/5 ml) and the homogenised suspension was centrifuged at 2,600 rpm for 10 min at 4°C in a J2-MC Beckman centrifuge. The supernatant was removed and recentrifuged at 26,000 rpm for 15 min at 4°C in a CS120GX micro ultracentrifuge (Hitachi). The pellet was resuspended in homogenisation buffer (100 µl/flask) and stored at –80°C in aliquots of 100 µl.

Protein measurement. The protein concentration of the samples was determined according to the method of Lowry [30] using bovine serum albumin as the standard.

Competition binding assays

Receptor binding assays were performed for Demotate in both rat brain cortex and AR42J cell membrane homogenates using [^{125}I-Tyr^3]octreotide (220 Ci/mmol) as the radioligand. Similar experiments were performed for [Tyr^3]octreotide and [Tyr^3]octreotate for comparison [14, 15, 16]. Typically, 30,000 cpm of radioligand was added in each test tube, containing rat brain cortex (corresponding to 50 µg protein) or AR42J cell membrane homogenate (corresponding to 10 µg protein) in the presence of increasing amounts of tested peptide in a total volume of 300 µl of 50 m*M* HEPES (pH 7.6, 0.3% BSA, 5 m*M* $MgCl_2$, 10 µ*M* Bacitracin). The samples were incubated for 40 min at 37°C and incubation was terminated by addition of ice-cold buffer (1 ml, 10 m*M* HEPES, 150 m*M* NaCl, pH 7.6). The suspension was rapidly filtered over glass fibre filters (Whatman GF/B, presoaked in binding buffer) on a Brandel Cell Harvester. The filters were rinsed thoroughly with buffer (4×2 ml) and filter activity was measured on an automatic NaI(TI) gamma counter. Non-specific binding was defined as the amount of activity still bound in the presence of 1 µ*M* [Tyr^3]octreotate. Binding data were analysed and IC_{50} values were calculated by non-linear regression according to a one-site model using the PRISM 2 program (Graph Pad Software, San Diego, Calif.).

Saturation binding assays

For saturation binding experiments [^{99g}Tc]Demotate was prepared in a similar manner as [^{99m}Tc]Demotate, employing a higher amount of $SnCl_2$. Both were purified by RP-HPLC and two sets of triplicates of the following concentrations were prepared (Tc peptide concentration = [^{99g}Tc]Demotate ± [^{99m}Tc]Demotate concentration) for total and non-specific binding, respectively: 0.06, 0.18, 0.42, 0.6, 1.8, 4.2, 6, 9, 12, 30, 60 and 300 n*M*. Saturation binding for [^{99m}Tc]Demotate was performed in rat brain cortex membrane homogenates as described previously [14]. Briefly, each assay tube contained 50 µl binding buffer (50 m*M* HEPES pH 7.6 containing 0.3% BSA, 10 m*M* $MgCl_2$, 14 mg/l Bacitracin), 50 µl radioligand solution of the corresponding concentration and 200 µl rat brain cortex membrane homogenate containing 40 µg protein. For the non-specific series, instead of 50 µl binding buffer, 20 µl binding buffer plus 30 µl 10 µ*M* [Tyr^3]octreotate solution was used. Tubes were incubated for 1 h at ambient temperature and then binding was interrupted by addition of 10 ml of ice-cold buffer (10 m*M* HEPES, 150 m*M* NaCl, pH 7.6) and rapid filtration through glass fibre filters (Whatman GF/B, presoaked in 0.3% BSA) on a Brandel Cell Harvester. Filter activity was measured on an automatic NaI(TI) gamma counter. Non-specific binding was defined as the amount of activity binding in the presence of 1 µ*M* [Tyr^3]octreotate. The Scatchard plot was then drawn and the K_d and B_{max} values were calculated employing the PRISM 2 program (GraphPad Software, San Diego, Calif.).

Internalisation experiments

For internalisation experiments AR42J cells were seeded at a density of 8×10^5 cells per well in six-well plates (Greiner Labortechnik, Germany) and grown to confluency for 48 h. On the day of the experiment, cells were washed twice with ice-cold internalisation medium prepared with F-12 K nutrient mixture supplemented by 1% (v/v) fetal bovine serum [31]. The cells were supplied with fresh medium (1.2 ml), and approximately 300,000 cpm [^{99m}Tc]Demotate (in 150 µl PBS/0.5% BSA buffer, corresponding roughly to 200 fmol total peptide) was added to the medium followed by PBS/0.5%BSA buffer alone (150 µl, total series) or with 10 µ*M* [Tyr^3]octreotate in PBS/0.5%BSA buffer (150 µl, non-specific series). The cells were incubated at 37°C in triplicates for each time point of 5-, 15-, 30-, 60- and 120-min incubation. Incubation was interrupted by removal of the medium and rapid rinsing with ice-cold internalisation medium two times. Thereafter, the cells were incubated twice at ambient temperature in acid wash buffer (50 m*M* glycine buffer pH 2.8, 0.1 *M* NaCl) for 5 min, a period reported to be sufficient for removal of more than 90% of membrane-bound radioligand [32, 33]. The supernatant was collected (membrane-bound radioligand fraction) and the cells were rinsed with PBS-0.5% BSA. Cells were lysed by treatment in 1 *N* NaOH and cell radioactivity collected (internalised radioligand fraction) [31]. Considering that total activity comprises membrane-bound plus internalised activity, the percent internalised activity versus the selected 5-, 15-, 30-, 60- and 120-min time intervals could be calculated applying the Microsoft Excel program.

Metabolic studies

Metabolic studies in murine plasma. For plasma stability studies, samples of [^{99m}Tc]Demotate were incubated at 37°C with freshly harvested murine plasma, and to aliquots withdrawn at 5, 15, 30 and 60 min time points EtOH was added in a 2/1 v/v EtOH/aliquot ratio. After centrifugation, supernatant samples were analysed by HPLC for metabolites applying the same conditions as for [^{99m}Tc]Demotate.

Metabolic studies in the urine. A 100-µl bolus containing >100 µCi [^{99m}Tc]Demotate was injected in the tail vein of Swiss Albino mice. The animals were kept for 30 min in metabolic cages with free access to water but not to food. They were sacrificed by cardiac puncture under a slight ether anaesthesia and the urine was withdrawn from the bladder with a syringe. This urine sample, as well as that collected in the metabolic cages within this period, was centrifuged at 35,000 rpm for 10 min and aliquots from the supernatant were analysed by HPLC applying the same conditions as for [^{99m}Tc]Demotate.

In vivo distribution experiments

In vivo distribution experiments in healthy mice. For tissue distribution experiments, male Swiss albino mice were each injected with a 100-µl bolus containing 4–5 µCi [^{99m}Tc]Demotate (corresponding to approx. 10 pmol of total peptide) via the tail vein. Animals were sacrificed in groups of five at 30-min and 1-, 2- and 4-h time points post injection (p.i.). Two additional groups of 30-min and 2-h intervals were injected intraperitoneally (i.p.) with 50 µg of [Tyr^3]octreotate prior to the injection of the radioligand (blocked animals). Alternatively, for blocked animals, 50 µg of [Tyr^3]octreotate was administered intravenously (i.v.) together with the radioligand. Blood and urine were immediately collected and organs of interest were excised, weighed and their radioactivity content measured in an automatic gamma counter using proper standards. Tissue distribution data were calculated as percent injected dose per organ (%ID/organ) and per gram (%ID/g) applying a suitable algorithm.

In vivo distribution experiments in AR42J tumour-bearing mice. In the flanks of each of 12 female Swiss-nu/nu mice, inocula (150 µl) containing a suspension of 0.8–1×10^7 AR42J cells in PBS buffer were subcutaneously (s.c.) injected. Tumours of substantial size were grown within 12 days, whereupon biodistribution experiments were performed. Six animals among the 12 were injected with 50 µg of [Tyr³]octreotate together with the radioligand via the tail vein and were used as the blocked animals. Mice were sacrificed at 1- and 4-h intervals p.i. and biodistribution studied as described above.

Imaging

The experimental AR42J tumour was grown in the femur of two athymic mice 2 weeks after inoculation. The animals were injected via the tail vein with a bolus containing [^{99m}Tc]Demotate (200 µCi, 200 µl) alone or together with 100 µg [Tyr³]octreotate (blocked animal) and were sacrificed 1 h p.i. by ether inhalation. They were placed in a typical position for planar imaging under a small field of view experimental gamma camera, suitable for both planar and tomographic imaging [24, 25]. For single-photon emission tomographic (SPET) imaging, the mouse was rotated with a computer-controlled step-motor and 36 planar images were acquired from 0° to 350° with a 10° step. An ordered subsets expectation maximisation algorithm was used for accurate reconstruction of tomographic slices. Acquisition time was 10 min in planar and 5 min per projection in tomographic mode. Correction for ^{99m}Tc decay was performed in projection data as well. Imaging was immediately followed by dissection of the animals for correlation of scintigraphic findings with anatomical and tissue distribution data.

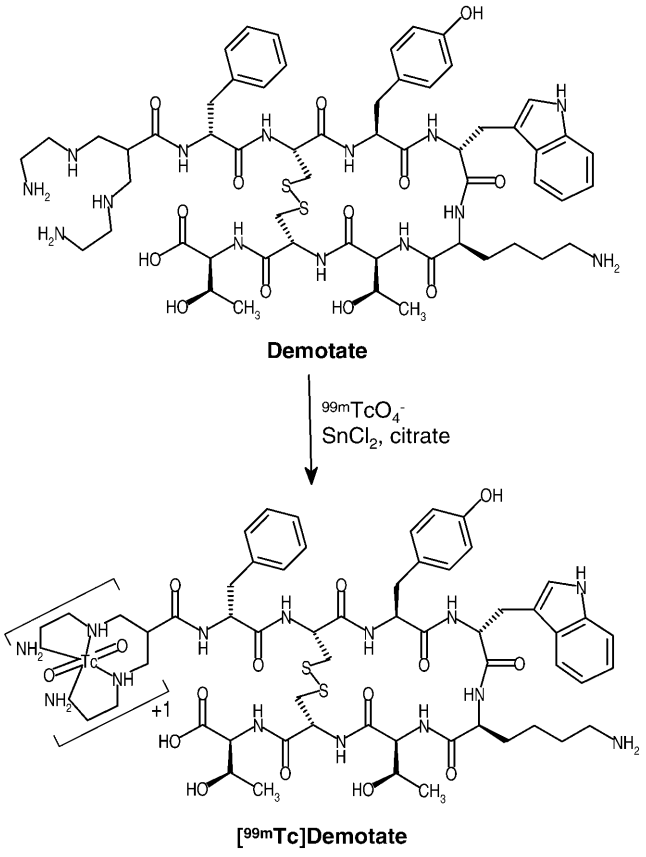

Fig. 1. Labelling of Demotate with ^{99m}Tc: formation of [^{99m}Tc]Demotate

Results

Synthesis of Demotate

The [Tyr³]octreotate amino acid sequence (D)Phe-Cys-Tyr-(D)Trp-Lys-Thr-Cys-Thr-OH was built on the solid support applying Fmoc and Boc protection strategies and the Boc-protected tetraamine ligand precursor was coupled to (D)Phe¹ by means of its 6-carboxylate anchor under formation of an amide bond. The [N_4^0, Tyr³]octreotate chain was cleaved from the solid support by TFA treatment that also removed all lateral protecting groups from the conjugate. Cyclisation in aqueous DMSO was followed by HPLC purification. The purity of the product was tested by analytical HPLC and the ES-MS data were consistent with the expected structure (Fig. 1).

Radiochemistry

Labelling of Demotate with ^{99m}Tc was performed in alkaline aqueous medium using stannous chloride in the presence of citrate for reduction of pertechnetate. Incorporation of the radiometal was practically quantitative within 30-min incubation at ambient temperature, leading to a single radioactive ^{99m}Tc species, [^{99m}Tc]Demotate (Fig. 1). Typically, 15 nmol peptide sufficed for complete incorporation of approximately 15 mCi $^{99m}TcO_4^-$, found in fresh generator eluate. The generator had been pre-eluted no longer than 24 h previously. Filtering the generator eluate through cation exchange cartridges with the purpose of removing all trace metals favoured labelling yields at higher specific activities. The specific activity could be further increased by using generator eluates obtained 3 h after previous elution, as in this way the ^{99g}Tc (carrier technetium) content was kept to a minimum [34, 35]. However, given that recent evidence has shown that the presence of a "critical mass" of unlabelled peptide significantly improves the cell internalisation properties as well as the localisation capability of peptide radioligands at the target tissue both in experimental animals and in patients [6], the typically achieved specific activity of 1 Ci/µmol peptide was considered satisfactory [13, 20]. As a consequence, further studies were conducted by employing [^{99m}Tc]Demotate as found in the neutralised labelling mixture and without further purification.

As indicated by HPLC analysis performed immediately after labelling, formation of [^{99m}Tc]Demotate was practically quantitative (Fig. 2). Paper chromatography analysis, performed in parallel, ruled out the formation

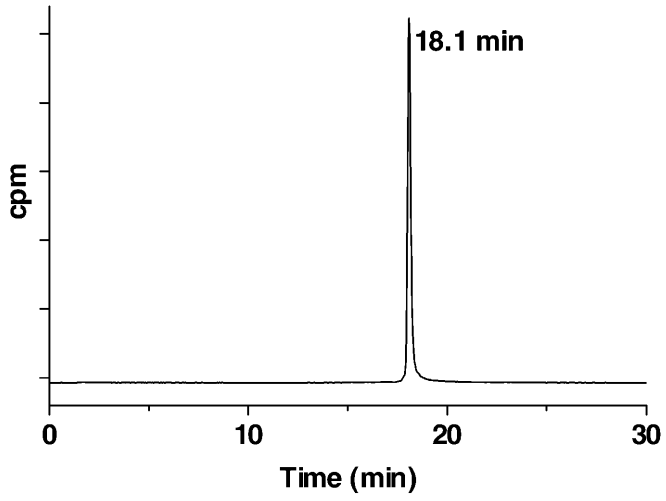

Fig. 2. Representative radiochromatogram of HPLC analysis of [^{99m}Tc]Demotate crude labelling reaction mixture

of reduced hydrolysed technetium. Stability HPLC tests carried out up to 6 h after labelling demonstrated that [^{99m}Tc]Demotate remained more than 96% intact during this period.

Binding properties of Demotate

Competition binding experiments were performed in membrane homogenates from rat brain cortex or from rat pancreatic carcinoma AR42J cells, predominantly expressing somatostatin subtype 2 receptors [36, 37, 38]. [^{125}I-Tyr^3]octreotide was used as the radioligand while [Tyr^3]octreotate and [Tyr^3]octreotide were the reference compounds. In both models the displacement studies revealed that Demotate, when compared with [Tyr^3]octreotate and [Tyr^3]octreotide, inhibited the binding of [^{125}I-Tyr^3]octreotide in a monophasic manner. Cumulative data from representative competition curves are shown in Fig. 3, demonstrating the high affinity of Demotate for somatostatin subtype 2 receptors.

Saturation binding of [^{99m}Tc]Demotate

Saturation binding data for [^{99m}Tc/^{99g}Tc]Demotate were acquired from experiments in rat brain cortex membranes and the saturation curve was plotted. Due to the high specific activity of ^{99m}Tc (520 Ci/μmol) [35], homogeneous peptide concentrations in the range 1–10 n*M* were reached by using a mixture of ^{99m}Tc + ^{99g}Tc radionuclides in the radioligand preparation. A clear concentration dependence of [^{99m}Tc/^{99g}Tc]Demotate binding to the rat brain cortex somatostatin receptors was demonstrated (Fig. 4). Fitting of the data to a one-site model was consistent with binding of [^{99m}Tc/^{99g}Tc]Demotate to a single class of binding sites. Scatchard transformation of the saturation curve was linear, demonstrating again the strong interaction of [^{99m}Tc/^{99g}Tc]Demotate with high-affinity binding sites in rat brain cortex membranes (Fig. 4, inset). The equilibrium dissociation constant K_d was 70 p*M* and the maximum binding capacity B_{max} reached 185 fmol/mg protein. This B_{max} value corresponds well to the data previously reported for rat brain cortex membranes [23]. The high binding affinity of [^{99m}Tc/^{99g}Tc]Demotate as compared with [^{111}In]OctreoScan (only IC_{50} values available [4, 39]) could be related to the positive versus negative charge of the respective metal chelates in the two compounds. In fact, an increase in the affinity in other somatostatin analogues that carry positively charged metal complexes has been reported [40].

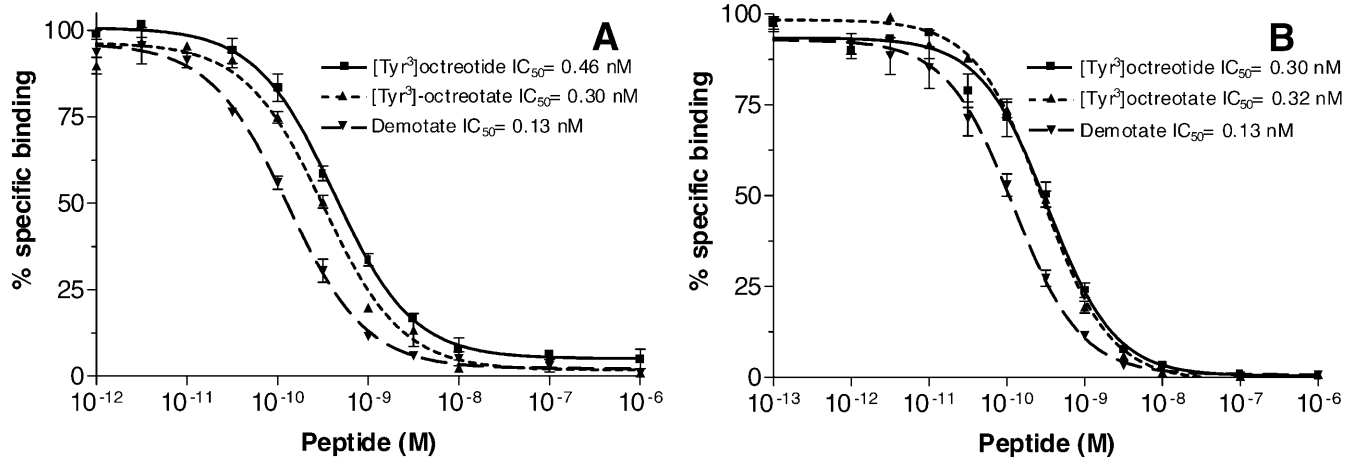

Fig. 3. Comparative displacement curves of [^{125}I-Tyr^3]octreotide from somatostatin binding sites by Demotate, [Tyr^3]octreotide and [Tyr^3]octreotate in: **A** rat brain cortex membrane preparations and **B** AR42J membrane homogenates

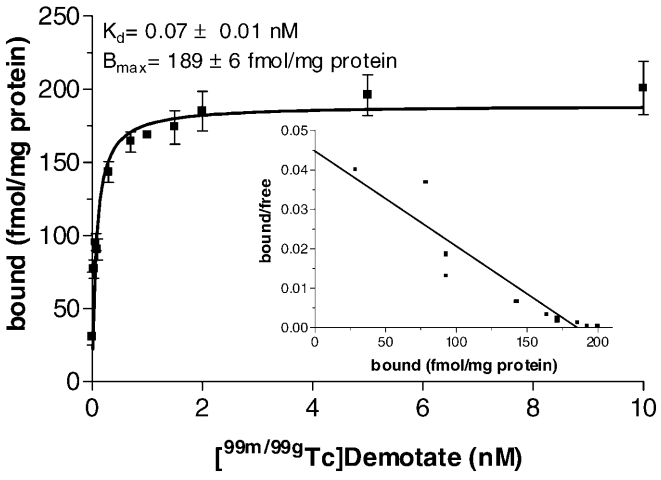

Fig. 4. Concentration dependence of [^{99m}Tc/^{99g}Tc]Demotate binding to rat brain cortex membranes. Specifically bound radioligand is plotted as a function of increasing concentrations of [^{99m}Tc/^{99g}Tc]Demotate. *Inset:* binding data plotted by the method of Scatchard. The maximum binding capacity (B_{max}) was calculated from the intercept on the abscissa and the affinity (K_d) from the slope of the line

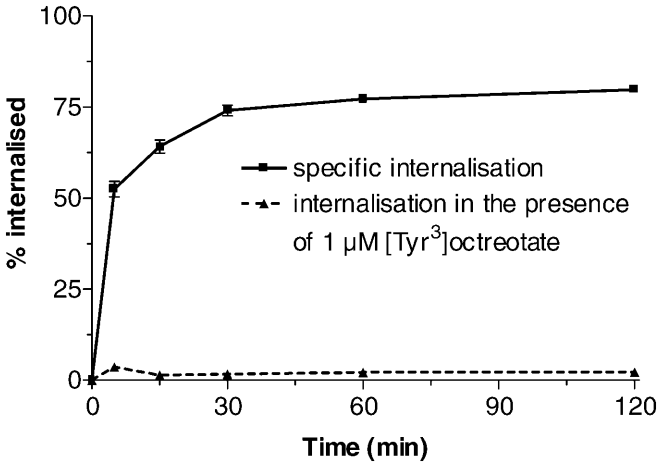

Fig. 5. Time course of the internalisation of [^{99m}Tc]Demotate in AR42J cells at 37°C. The internalisation percentage was determined by dividing acid-resistant binding by total specific binding. Data represent the mean values of three independent experiments in triplicate.

Internalisation

The internalisation properties of [^{99m}Tc]Demotate were studied in AR42J cells over time. The cells were incubated at 37°C with the radioligand with or without addition of a high excess of [Tyr^3]octreotate (non-specific series). Radioactivity bound to the receptor on the membrane was "acid washed" with glycine buffer, pH 2.8 (membrane-bound activity), whereas radioactivity in the cell (internalised activity) was collected after lysing the cells by treatment with 1 *N* NaOH. The curve of percent internalised activity versus the selected time points could be drawn (Fig. 5), revealing that [^{99m}Tc]Demotate rapidly reaches an internalisation plateau of 80% within the first 15 min of incubation in AR42J cells.

Metabolic stability of [^{99m}Tc]Demotate

By incubation of [^{99m}Tc]Demotate in fresh murine plasma at 37°C and HPLC analysis of incubates at selected time points, the resistance of the radiopeptide to enzymatic degradation was established. Furthermore, by HPLC analysis of urine collected 30 min after i.v. injection of [^{99m}Tc]Demotate in mice, all radioactivity could be assigned to [^{99m}Tc]Demotate, demonstrating again the high in vivo stability of this compound.

Body distribution of [^{99m}Tc]Demotate

Soon after administration, [^{99m}Tc]Demotate was rapidly cleared from the blood and the body of mice into the urine via the kidneys and the urinary tract as a result of its high hydrophilicity (Fig. 6A). Significant uptake was found in the pancreas, the adrenals and the gastrointestinal tract (stomach and intestines), where the somatostatin binding sites are located (Fig. 6B). This uptake was proved to be somatostatin receptor mediated, as in the groups of blocked animals it was found to be substantially reduced. The initial high radioactivity uptake in the pancreas diminished over time, probably due to the excessive enzymatic activity in this organ. Uptake in the liver was minimal at all time points, further suggesting that the high stomach and observed intestine uptake of [^{99m}Tc]Demotate is receptor specific and not related to a hepatobiliary excretion of the radioligand. In fact, the kidneys and the urinary system represent the predominant excretion route for [^{99m}Tc]Demotate. As the background activity gradually cleared from the body, the target to non-target ratios increased (Fig. 6C). These values demonstrate the excellent pharmacokinetic profile of [^{99m}Tc]Demotate and constitute a significant improvement over other ^{99m}Tc-tetraamine-modified somatostatin analogues [16].

Tumour uptake of [^{99m}Tc]Demotate

Results of [^{99m}Tc]Demotate tissue distribution studies in athymic mice bearing the AR42J experimental tumour are summarised in Fig. 7A as %ID/g. These data show the high tumour accumulation of [^{99m}Tc]Demotate (25%ID/g) at 1 h p.i. that remains high (20%ID/g) up to 4 h p.i. This uptake could be significantly blocked (by >90%) in the animals receiving a high dose of cold pep-

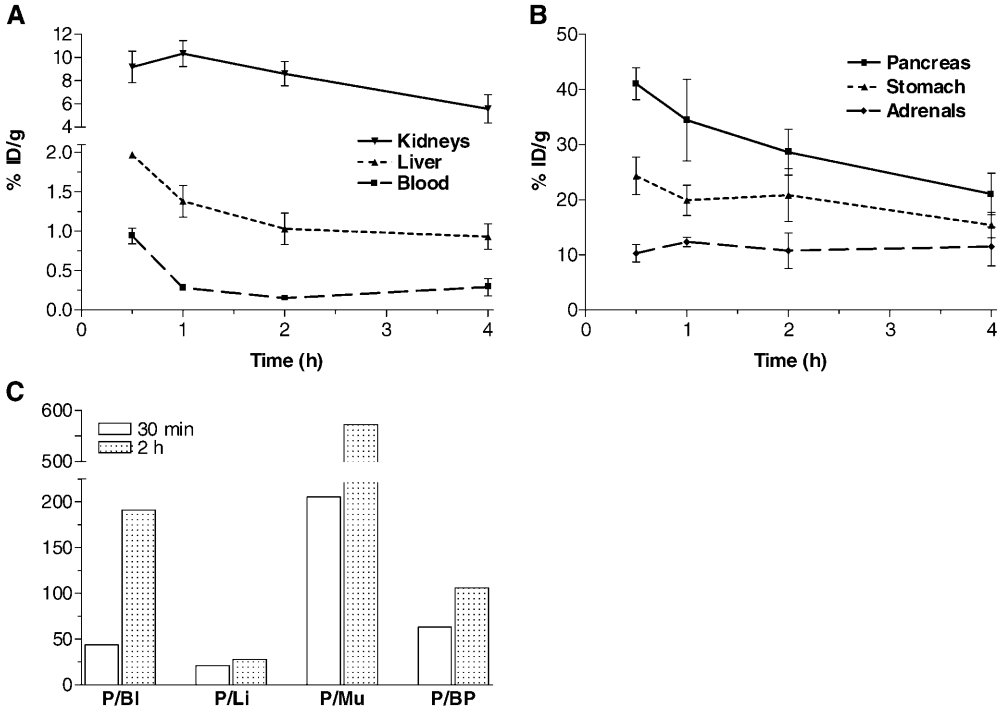

Fig. 6. A Washout of [^{99m}Tc]Demotate from blood through the kidneys and the liver of healthy mice at 30 min and 1, 2 and 4 h p.i. **B** Uptake in somatostatin receptor-rich organs, the pancreas, adrenals and stomach, at the same time points. **C** Target to background ratios for [^{99m}Tc]Demotate at 30 min and 2 h p.i. Data represent %ID/g values and are the mean of results from four to six animals per time point. *P*, Pancreas; *Bl*, blood; *Li*, liver; *Mu*, muscle; *BP*, blocked pancreas

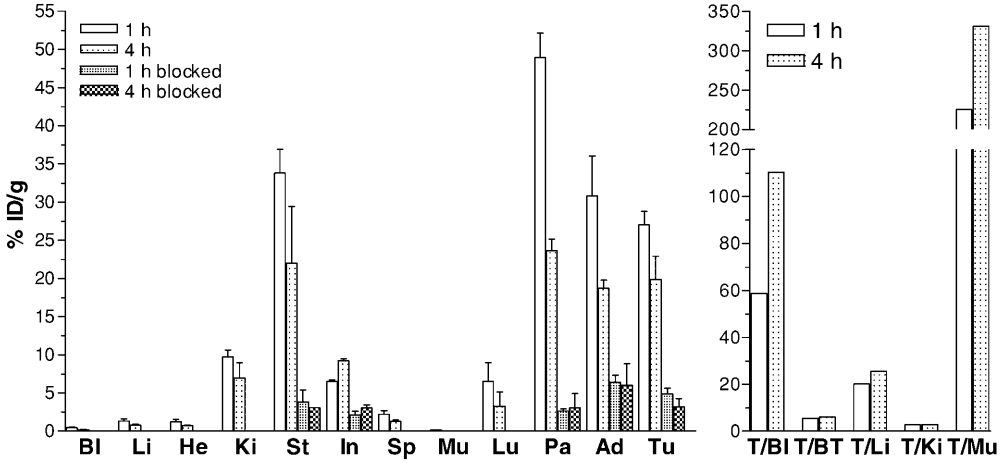

Fig. 7. *Left:* Tissue distribution data of [^{99m}Tc]Demotate in AR42J tumour-bearing athymic mice at 1 and 4 h p.i. Data represent %ID/g values and are the mean of results from four animals per time point. *Bl*, Blood; *Li*, liver; *He*, heart; *Ki*, kidneys; *St*, stomach; *In*, intestines; *Sp*, spleen; *Mu*, muscle; *Lu*, lung; *Pa*, pancreas; *Ad*, adrenals; *Tu*, AR42J tumour. *Right:* Tumour (*T*) to background ratios of [^{99m}Tc]Demotate at 1 and 4 h p.i. *BT*, Blocked tumour

tide together with the radioligand and can therefore be considered as receptor specific. As the background activity dropped with time, the target to non-target ratios (tumour to blocked tumour, tumour to blood, tumour to liver and tumour to muscle) already high at 1 h p.i. increased even further at 4 h p.i., while the tumour to kidney ratio remained unaltered (Fig. 7B).

Imaging

Static images of two athymic mice bearing the AR42J experimental tumour in the femur area are presented in Fig. 8A, while SPET images are shown in Fig. 8B. As shown by the planar images, the excellent clearing properties of [^{99m}Tc]Demotate are evident in both animals. Clear delineation of the tumour in the animal receiving the radioligand alone is achieved, and in combination with the rapid body clearance this results in a high-quality image. In the animal receiving a high dose of [Tyr^3]octreotate together with the radioligand, the tumour is totally blocked, while some activity is still found in the kidneys. SPET imaging provided accurate information on [^{99m}Tc]Demotate 3D distribution within the tumour. The images of six successive slices (at 1-mm intervals) within the tumour reveal several hot spots (Fig. 8B), indicating that the tumour is non-homogeneous in morphology and function. Fifteen such slices were used for 3D tumour reconstruction, and four such images, each from a different viewing point, are presented in Fig. 8C. The red colour corresponds to high activity and the yellow colour to lower activity (necrotic) areas inside

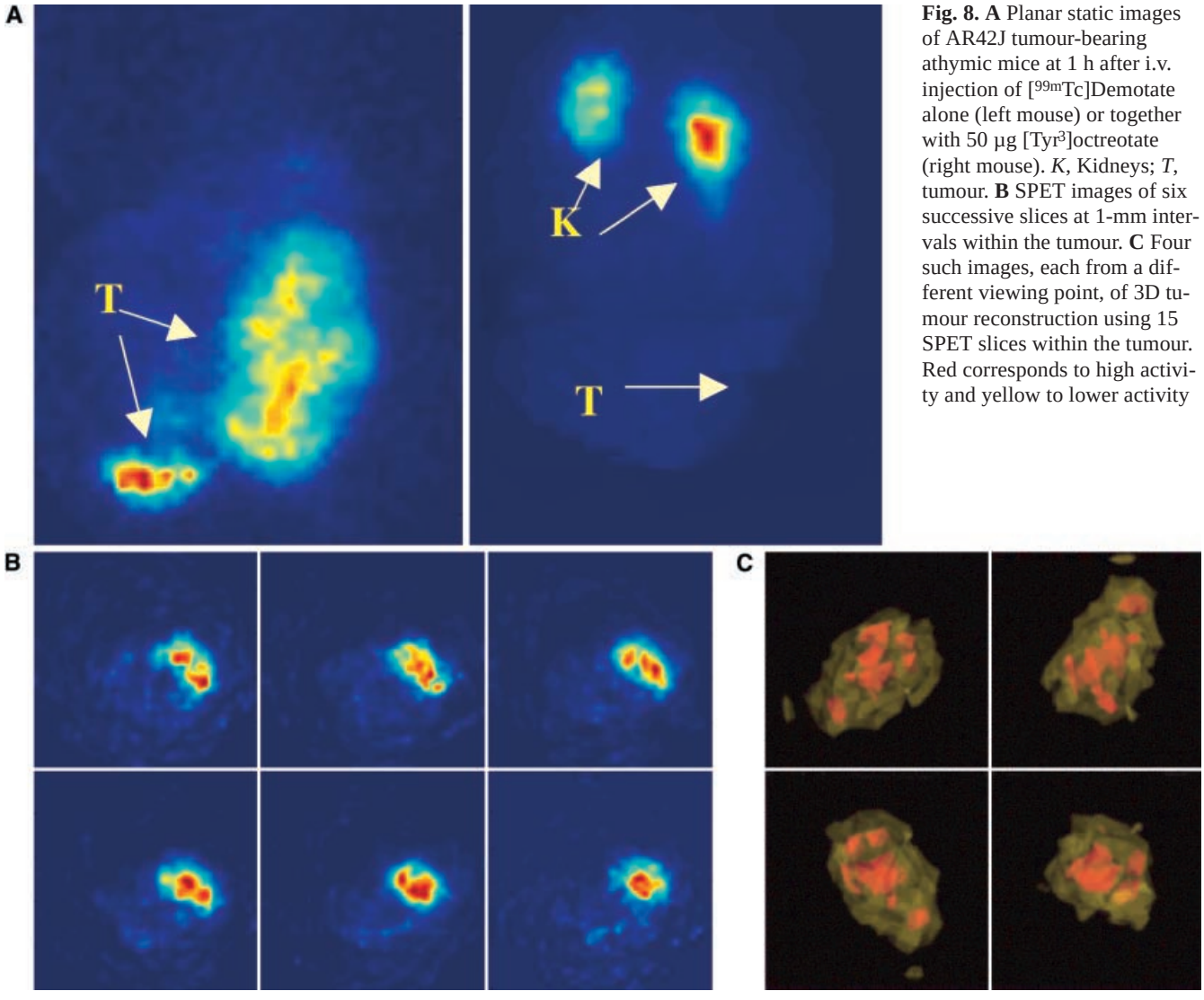

Fig. 8. A Planar static images of AR42J tumour-bearing athymic mice at 1 h after i.v. injection of [^{99m}Tc]Demotate alone (left mouse) or together with 50 µg [Tyr^3]octreotate (right mouse). *K*, Kidneys; *T*, tumour. **B** SPET images of six successive slices at 1-mm intervals within the tumour. **C** Four such images, each from a different viewing point, of 3D tumour reconstruction using 15 SPET slices within the tumour. Red corresponds to high activity and yellow to lower activity

the tumour, well delineated in 3D reconstruction. The non-homogeneous morphology of this tumour model was confirmed by tumour dissection following imaging.

Discussion

This work reports on the synthesis and preclinical evaluation of a novel ^{99m}Tc-based somatostatin analogue – [^{99m}Tc]Demotate – with potential use in the visualisation of somatostatin receptor-positive tumours and their metastases. Despite the fact that several somatostatin analogues labelled with a wide spectrum of radionuclides have already been reported [4, 6, 8, 39, 40] and an established radiopharmaceutical, [^{111}In]OctreoScan, is available [4, 10], the search for a ^{99m}Tc somatostatin radiotracer has been intensified [3, 5, 11, 12, 13, 14, 15, 16, 17, 18, 19, 20]. Due to the superior nuclear properties of ^{99m}Tc and its cost-effectiveness, a somatostatin receptor-seeking ^{99m}Tc compound constitutes a highly attractive alternative to [^{111}In]OctreoScan in routine nuclear medicine diagnosis [3, 5].

Previous efforts to develop such an agent have mainly utilised octreotide/[Tyr^3]octreotide as the somatostatin receptor recognition site. A variety of chelators attached to the N-terminal of the octapeptide and serving as the radiometal binding site have been tested. Peptide modifications with HYNIC or open chain tetraamines have so far given the best results in terms of tissue distribution profiles and tumour-targeting properties [3, 5, 11, 12, 13, 14, 15, 16, 17, 18, 19, 20].

In the present work, which can be considered a continuation of previous work [15, 16], [Tyr^3]octreotate was the peptide of choice. Substitutions of Phe^3 by Tyr^3 and Thr(ol)^8 by Thr^8 in the original octreotide motif were expected to increase the hydrophilicity and thereby to improve the in vivo performance of the final ^{99m}Tc radioligand. This decision was further supported by recent evi-

dence reporting on the superior tumour localisation properties of [Tyr^3]octreotate versus octreotide/[Tyr^3]octreotide analogues carrying identical metal chelates [4, 6, 8, 21, 22, 40].

A tetraamine derivative was selected as the ^{99m}Tc binding site. This chelator, an improved version of a previously reported agent [16], contains a carboxylic anchor that facilitates the direct coupling of the tetraamine backbone to [Tyr^3]octreotate under formation of an amide bond. In this way, the cumbersome multistep synthesis of previously reported tetraamine precursors [16] was shortened to a mere two-step process, while the omission of benzyl group(s) containing spacers was expected to further increase the hydrophilicity of the final compound and accelerate its washout from non-target regions of the body.

Labelling with ^{99m}Tc was accomplished by simply mixing generator eluate with a buffered solution containing Demotate, tin chloride and citrate and briefly incubating this mixture at ambient temperature. Incorporation of the radiometal by the open chain tetraamine was practically quantitative, leading to a single radioactive species, [^{99m}Tc]Demotate. As previously reported, the forming [^{99m}Tc]tetraamine complex is a monocationic $Tc(V)O_2^+$ species adopting an octahedral structure [41, 42, 43, 44] and showing a high kinetic stability and a high hydrophilicity [45, 46]. The established structure of this complex may present clear advantages if product commercialisation and licence by official authorities are planned. Specific activities of 1 Ci ^{99m}Tc/µmol peptide could be routinely reached, which is within the range of values reported for satisfactory somatostatin receptor targeting applications with ^{99m}Tc [13, 20]. Therefore, and in contrast to what was originally reported for [^{99m}Tc-N_4^0]octreotide [16], purification of the labelling reaction mixture by HPLC was not necessary. Nevertheless, [^{99m}Tc]Demotate in higher specific activities could be obtained by carefully monitoring the amount of metal traces in the labelling reaction mixture. As demonstrated by in vitro and in vivo tests following labelling, [^{99m}Tc]Demotate retained its receptor affinity (vide infra). This fact strongly suggests that the disulphide bridge of the octapeptide remained unaffected by the reduction conditions of the labelling process [11]. The easy formation of [^{99m}Tc]Demotate, which does not require heating of the labelling mixture, and its stability in the open vial for at least 6 h following labelling present clear practical advantages for future routine application of [^{99m}Tc]Demotate in a clinical environment. The resistance of [^{99m}Tc]Demotate to enzymatic degradation in plasma and the fact that it is excreted intact into the urine reflect its stability also in the biological milieu.

Unlabelled Demotate displayed high-affinity binding to somatostatin receptors (IC_{50}=0.13 n*M*) comparable to that of [Tyr^3]octreotide and [Tyr^3]octreotate. On the other hand, [^{99m}Tc]Demotate showed selectivity and high affinity for somatostatin receptors in vitro (K_d=0.07 n*M*) and internalised very rapidly in cell lines expressing somatostatin subtype 2 receptors. In agreement with the in vitro findings, in vivo tests demonstrated the high and specific localisation of [^{99m}Tc]Demotate in somatostatin receptor-rich tissues, both normal and neoplastic. Thus, high and specific uptake in the pancreas, adrenals, stomach and intestine was found for both animal species used in this study (healthy Swiss albino mice and the tumour-bearing nude/nude mice). The presence of [Tyr^3]octreotate moiety in combination with the monocationic [$^{99m}TcO_2$]N$^+$ metal chelate seems to have a synergic effect in improving the localisation properties of [^{99m}Tc]Demotate by increasing the receptor affinity and internalisation rate of the radiopeptide. In fact, similar effects have been reported for other [Tyr^3]octreotate analogues [4, 6, 8, 21, 22, 40]. Very high uptake by the experimental tumour (~25%ID/g) was seen at 1 h p.i. and this uptake remained high (~20%ID/g) up to 4 h p.i., while results from in vivo blocking experiments ruled out a non-specific accumulation. The 20%ID/g value at 4 h p.i. is at least twice as high as the corresponding values reported for [^{99m}Tc-HYNIC^0,Tyr^3]octreotide analogues applying the same animal model [18]. Using EDDA, tricine-nicotinic acid or tricine co-ligands, the reported AR42J tumour %ID/g values for the corresponding [^{99m}Tc-HYNIC] radiopeptides are 9.65, 5.80 and 9.58 at 4 h p.i. Again, the use of [Tyr^3]octreotate in this study instead of [Tyr^3]octreotide [18], along with the monocationic metal chelate residue [40], seems to have been responsible for this difference.

The high and specific localisation of [^{99m}Tc]Demotate in somatostatin binding sites in vivo was paralleled by a very rapid washout of this agent from all non-target regions of the body via the kidneys into the bladder. As a result, high target to background ratios were exhibited by [^{99m}Tc]Demotate, illustrating the favourable characteristics of this agent for imaging. These promising properties were clearly evident in the high-quality images obtained 1 h after administration of [^{99m}Tc]Demotate in animal models.

In conclusion, the new radioligand reported herein, [^{99m}Tc]Demotate, combines the advantages of high affinity, rapid target localisation and fast body clearance. Furthermore, the wide availability of ^{99m}Tc makes [^{99m}Tc]Demotate a highly attractive tracer for the diagnostic imaging of somatostatin receptor-positive tumours in patients. This is further supported by the fact that, due to the high photon flux of ^{99m}Tc, the patient's whole-body dose can be markedly reduced by using this short-lived radionuclide in combination with a small and rapidly localising molecule without compromising image quality. Further studies for the validation of [^{99m}Tc]Demotate in a small number of carcinoid and pancreatic carcinoma patients are currently in progress.

Acknowledgements. We thank Mrs. C. Tsipra and Dr. M. Poppe for their contribution in the preparation of the bifunctional tetraamine precursor and Dr. L. Leondiades for the ES-MS spectra. We also thank Dr. S. Mather, Prof. H. Mäcke, Dr. B. Stolz, Dr. D. Yannoukakos and H. Georgoussi for sharing their experience with the in vitro tests.

This work was supported by the General Secretariat for Research and Technology of Greece through the National Program EPET II: "Cancer Biology: Genetic Analysis and In Vivo Receptor Imaging – Radiotherapy" (Project No.: 97EKBAN2-1,2-112) and by the International Atomic Energy Agency through the Coordination Research Program: "^{99m}Tc-Labelled Peptides for Imaging of Peripheral Receptors" (Contract No.: 8967/R0; Regular Budget Fund).

References

1. Fischman AJ, Babich JW, Strauss HW. A ticket to ride: peptide radiopharmaceuticals. *J Nucl Med* 1993; 34:2253–2263.
2. Reubi JC. Neuropeptide receptors in health and disease: the molecular basis for in vivo imaging. *J Nucl Med* 1995; 36: 1825–1835.
3. Liu S, Edwards DS, Barrett JA. ^{99m}Tc labeling of highly potent small peptides. *Bioconjug Chem* 1997; 8:621–636.
4. de Jong M, Breeman WAP, Bakker WH, Kooij PPM, Bernard BF, Hofland LJ, Visser TJ, Srinivasan A, Schmidt MA, Erion JL, Bugai JE, Mäcke HR, Krenning EP. Comparison of ^{111}In-labeled somatostatin analogs for tumor scintigraphy and radionuclide therapy. *Cancer Res* 1998; 58:437–441.
5. Liu S, Edwards DS. ^{99m}Tc-labeled small peptides as diagnostic radiopharmaceuticals. *Chem Rev* 1999; 99:2235–2268.
6. Breeman WAP, de Jong M, Kwekkeboom DJ, Valkema R, Bakker WH, Kooij PPM, Visser TJ, Krenning EP. Somatostatin receptor-mediated imaging and therapy: basic science, current knowledge, limitations and future perspectives. *Eur J Nucl Med* 2001; 28:1421–1429.
7. Lamberts SW, Krenning EP, Reubi JC. The role of somatostatin and its analogs in the diagnosis and treatment of tumors. *Endocr Rev* 1991; 12:450–482.
8. Reubi JC, Schar JC, Waser B, Wenger S, Heppeler A, Schmitt JS, Mäcke HR. Affinity profiles for human somatostatin receptor subtypes SST1–SST5 of somatostatin radiotracers selected for scintigraphic and radiotherapeutic use. *Eur J Nucl Med* 2000; 27:273–282.
9. Bakker WH, Krenning EP, Breeman Kooij PPM, Reubi JC, Koper JW, de Jong M, Lameris JS, Visser TJ, Lamberts SW. In vivo use of a radioiodinated somatostatin analog: dynamics, metabolism and binding to somatostatin receptor-positive tumors in man. *J Nucl Med* 1991; 32:1184–1189.
10. Krenning EP, Bakker WH, Kooij PPM, Breeman WAP, Oei HY, de Jong M, Reubi JC, Visser TJ, Bruns C, Kwekkeboom DJ, Reijs AEM, van Hagen PM, Koper JW, Lamberts SWJ. Somatostatin receptor scintigraphy with indium-111-DTPA-D-Phe-1-octreotide in man: metabolism, dosimetry and comparison with iodine-123-Tyr-3-octreotide. *J Nucl Med* 1992; 33:652–658.
11. Vallabhajosula S, Moyer BR, Lister-James J, McBride WJ, Lipszyc H, Lee H, Bastidas D, Dean RT. Preclinical evaluation of technetium-99m-labeled somatostatin receptor binding peptides. *J Nucl Med* 1996; 37:1016–1022.
12. Pearson DA, Lister-James J, McBride WJ, Wilson DM, Martel LJ, Civitello ER, Taylor JE, Moyer BR, Dean RT. Somatostatin receptor-binding peptides labeled with technetium-99m: chemistry and initial biological studies. *J Med Chem* 1996; 39:1361–1371.
13. Blum J, Handmaker H, Lister-James J, Rinne N. A multicenter trial with a somatostatin analog ^{99m}Tc depreotide in the evaluation of solitary pulmonary nodules. *Chest* 2000; 117:1232–1238.
14. Decristoforo C, Mather SJ. Preparation, ^{99m}Tc-labeling and in vitro characterisation of HYNIC and N_3S modified RC-160 and [Tyr^3]octreotide. *Bioconjug Chem* 1999; 10:431–438.
15. Maina T, Stolz B, Albert R, Bruns C, Koch P, Mäcke H. Synthesis, radiochemistry and biological evaluation of a new somatostatin analog (SDZ 219–387) labeled with technetium-99m. *Eur J Nucl Med* 1994; 21:437–444.
16. Maina T, Stolz B, Albert R, Nock B, Bruns C, Mäcke H. Synthesis, radiochemical and biological evaluation of ^{99m}Tc[N_4-(D)Phe^1]octreotide, a new octreotide derivative with high affinity for somatostatin receptors. In: Nicolini M, Bandoli G, Mazzi U, eds. *Technetium and rhenium in chemistry and nuclear medicine, 4*. Padova: SG Editoriali; 1995:395–400.
17. Thakur ML, Kolan H, Li J, Wiaderkiewicz R, Pallela VR, Duggaraju R, Schally AV. Radiolabeled somatostatin analogs in prostate cancer. *Nucl Med Biol* 1997; 24:105–113.
18. Decristoforo C, Melendez-Alafort L, Sosabowski JK, Mather SJ. ^{99m}Tc-HYNIC-[Tyr^3]-octreotide for imaging somatostatin-receptor-positive tumors: preclinical evaluation and comparison with ^{111}In-octreotide. *J Nucl Med* 2000; 41:1114–1119.
19. Decristoforo C, Mather SJ, Cholewinski W, Donnemiller E, Riccabona G, Moncayo R. ^{99m}Tc-EDDA/HYNIC-TOC: a new ^{99m}Tc-labeled radiopharmaceutical for imaging somatostatin receptor-positive tumors: first clinical results and intra-patient comparison with ^{111}In-labeled octreotide derivatives. *Eur J Nucl Med* 2000; 27:1318–1325.
20. Bangard M, Béhé M, Guhlke S, Otte R, Bender H, Mäcke HR, Biersack HJ. Detection of somatostatin receptor-positive tumours using the new ^{99m}Tc-tricine-HYNIC-D-Phe^1-Tyr^3-octreotide: first results in patients and comparison with ^{111}In-DTPA-D-Phe^1-octreotide. *Eur J Nucl Med* 2000; 27:628–637.
21. Erion JL, Srinivasan A, Schmidt MA, Wilhelm R, Bugaj JE. Radiolabeled ligand-octreotate conjugates: evaluation of potential diagnostic and therapeutic radiopharmaceutical agents targeted to somatostatin receptors. *J Nucl Med* 1997; 38:190P.
22. Kwekkeboom DJ, Bakker WH, Kooij PPM, Konijnenberg MW, Srinivasan A, Erion JL, Schmidt MA, Bugaj JL, de Jong M, Krenning EP. [^{177}Lu-DOTA^0,Tyr^3]octreotate: comparison with [^{111}In-DTPA^0]octreotide in patients. *Eur J Nucl Med* 2001; 28:1319–1325.
23. Bakker WH, Krenning EP, Breeman WAP, Koper JW, Kooij PP, Reubi JC, Klijn JG, Visser TJ, Docter R, Lamberts S. Receptor scintigraphy with a radioiodinated somatostatin analog: radiolabeling, purification, biologic activity and in vivo application in animals. *J Nucl Med* 1990; 31:1501–1509.
24. Loudos GK, Nikita KS, Mouravliansky NA, Uzunoglu NK, Matsopoulos GK, Giokaris ND, Karabarbounis A, Papanicolas CN, Styliaris E, Archimandritis SC, Varvarigou AD, Maintas D, Stefanis K. An assessment of position sensitive photomultiplier tubes for high resolution 3D imaging. Proceedings of IEEE, Nuclear Science Symposium and Medical Imaging, Lyon 2000: in press.
25. Loudos G, Nikita K, Uzunoglu N, Mouravliansky N, Matsopoulos G. Performance of iterative reconstruction algo-

rithms for small organs high resolution SPECT imaging using a PSPMT based detector [abstract]. *Eur J Nucl Med* 2001; 28:970.
26. Barlos K, Gatos D, Kallitsis J, Papaphotiou G, Sotiriou P, Wenquing Y, Shafer W. Darstellung geschützter Peptid-fragmente unter Einsatz substituierter Triphenylmethyl-harze. *Tetrahedron Lett* 1989; 30:3943–3946.
27. Fields GB, Noble RL. Solid phase peptide synthesis utilizing 9-fluorenylmethoxycarbonyl amino acids. *Int J Pept Protein Res* 1990; 35:161–214.
28. Miranda LP, Alewood PF. Accelerated chemical synthesis of peptides and small proteins. *Proc Natl Acad Sci USA* 1999; 96:1181–1186.
29. Raynor K, Reisine T. Analogs of somatostatin selectively label distinct subtypes of somatostatin receptors in rat brain. *J Pharmacol Exp Ther* 1989; 251:510–517.
30. Lowry OH, Rosebrough NJ, Farr AL, Randall J. Protein measurement with the folin phenol reagent. *J Biol Chem* 1951; 193:265–275.
31. García-Garayoa E, Allemann-Tannahill L, Bläuenstein P, Willmann M, Carrel-Rémy N, Tourwé D, Iterbeke K, Conrath P, Schubiger PA. In vitro and in vivo evaluation of new radiolabeled neurotensin(8–13) analogs with high affinity for NT1 receptors. *Nucl Med Biol* 2001; 28:75–84.
32. Koenig JA, Edwardson JM, Humphrey PPA. Somatostatin receptors in Neuro2A neuroblastoma cells: ligand internalization. *Br J Pharmacol* 1997; 120:52–59.
33. Koenig JA, Kaur R, Dodgeon I, Edwardson JM, Humphrey PPA. Fates of endocytosed somatostatin sst_2 receptors and associated agonists. *Biochem J* 1998; 336:291–298.
34. Deutsch E, Heineman WR, Zodda JP, Gilbert TW, Williams CC. Preparation of "no-carrier-added" technetium-99m complexes: determination of the total technetium content of generator eluents. *Int J Appl Radiat Isot* 1982; 33:843–848.
35. Kowalsky RJ, Perry RJ. *Radiopharmaceuticals in nuclear medicine practice*. Norwalk, Conn.: Appleton & Lange; 1987:68.
36. Taylor JE, Theveniau MA, Bashirzadeh R, Reisine T, Eden PA. Detection of somatostatin receptor subtype 2 (SSTR2) in established tumors and tumor cell lines: evidence for SSTR2 heterogeneity. *Peptides* 1994; 15:1229–1236.
37. Froidevaux S, Hintermann E, Török M, Mäcke HR, Beglinger C, Eberle AN. Differential regulation of somatostatin receptor type 2 (sst 2) expression in AR4-2J tumor cells implanted into mice during octreotide treatment. *Cancer Res* 1999; 59: 3652–3657.
38. Froidevaux S, Heppeler A, Eberle AN, Meier A-M, Häusler M, Berglinger C, Béhé M, Powell P, Mäcke HR. Preclinical comparison in AR4-2J tumor-bearing mice of four radiolabeled 1,4,7,10-tetraazacyclododecane-1,4,7,10-tetraacetic acid-somatostatin analogs for tumor diagnosis and internal radiotherapy. *Endocrinology* 2000; 141:3304–3312.
39. Bakker WH, Albert R, Bruns C, Breeman WAP, Hofland LJ, Marbach P, Pless J, Pralet D, Stolz B, Koper JW, Lamberts SWJ, Visser TJ, Krenning EP. [^{111}In-DTPA-D-Phe^1]-octreotide, a potential radiopharmaceutical for imaging of somatostatin receptor-positive tumors: synthesis, radiolabeling and in vitro validation. *Life Sci* 1991; 49:1583–1591.
40. Lewis JS, Lewis MR, Srinivasan A, Schmidt MA, Wang J, Anderson CJ. Comparison of four ^{64}Cu-labeled somatostatin analogs in vitro and in a tumor-bearing rat model: evaluation of new derivatives for positron emission tomography imaging and targeted radiotherapy. *J Med Chem* 1999; 42:1341–1347.
41. Blake AJ, Greig JA, Schröder M. Rhenium complexes of tetraaza macrocycles: the synthesis and single-crystal X-ray structure of *trans*-[$Re(O)_2$(cyclam)]Cl·2(BPh_3·H_2O). *J Chem Soc Dalton Trans* 1988; 2645–2647.
42. Zuckman SA, Freeman GM, Troutner DE, Volkert WA, Holmes RA, Van Derveer DG, Barefield EK. Preparation and X-ray structure of *trans*-dioxo(1,4,8,11-tetraazacyclotetradecane)technetium(V) perchlorate hydrate. *Inorg Chem* 1981; 20:2386–2389.
43. Kastner ME, Lindsay MJ, Clarke MJ. Synthesis and structure of *trans*-[$O_2(en)_2Tc^V$]$^+$. *Inorg Chem* 1982; 21:2037–2040.
44. Parker D, Roy PS. Synthesis and characterization of stable rhenium(V) dioxo complexes with acyclic tetraamine ligands, [$LReO_2$]$^+$. *Inorg Chem* 1988; 27:4127–4130.
45. Herzog KM, Deutsch E, Deutsch K, Silberstein EB, Sarangarajan R, Cacini W. Synthesis and renal excretion of technetium-99m-labeled organic cations. *J Nucl Med* 1992; 33:2190–2195.
46. Bläuenstein P, Pfeiffer G, Schubiger PA, Anderegg G, Zollinger K, May K, Proso Z, Ianovici E, Lerch P. Chemical and biological properties of a cationic Tc-tetraamine complex. *Int J Appl Radiat Isot* 1985; 36:315–317.